

Calcia-doped yttria-stabilized zirconia for thermal barrier coatings: synthesis and characterization

Anup K. Bhattacharya · Patrick Reinhard ·
Walter Steurer · Valery Shklover

Received: 1 November 2010/Accepted: 4 April 2011/Published online: 20 April 2011
© Springer Science+Business Media, LLC 2011

Abstract Doping with other oxides has been a stabilization method of ZrO_2 for thermal barrier coating applications. Such a stabilized system is 7–8 mol% $\text{YO}_{1.5}$ -doped zirconia (7YSZ), which has been in use for around 20 years. In this study, calcia (CaO) and yttria (Y_2O_3) have been used for doping ZrO_2 to produce a stable single-phase cubic calcia-doped yttria-stabilized zirconia (CaYSZ). This has been synthesized using wet chemical synthesis as well as by solid-state synthesis. Unlike partially stabilized zirconia where 5 mol% CaO is doped into ZrO_2 , CaYSZ has been found to be stable up to 1600 °C. Detailed CaYSZ synthesis steps and phase characterization are presented. Wet chemical synthesis resulted in a stable single-phase CaYSZ just after 4 h treatment at 1400 °C, whereas a 36 h annealing at 1600 °C is required for CaYSZ synthesis during solid-state processing. The CaYSZ has been found stable even for 600 h at 1250 °C. Coefficient of thermal expansion and sintering temperature of CaYSZ was found to be $11 \times 10^{-6} \text{ K}^{-1}$ and 1220 °C, respectively, which are comparable to 7YSZ. An increase in sintering rate with increasing dopant concentration has also been observed.

Introduction

Development of new thermal barrier coatings (TBC) is necessary to improve turbine efficiency and to reduce gas emissions, without increasing the surface temperature of

the superalloy substrate components. Partially stabilized zirconia (PSZ) with 7–8 mol% $\text{YO}_{1.5}$ -doped zirconia (7YSZ) is the mostly used TBC material in high-efficient gas turbines, due to its good balance of mechanical and thermal properties. Application of 7YSZ is however limited to operation temperatures of ~ 1150 °C [1] and it also corrodes at high temperature [2]. 7YSZ formed under plasma spray conditions or during electron-beam physical vapor deposition exists as a metastable, “non-transformable”, t' phase at room temperature [3, 4]. The lifetime of 7YSZ is limited when used for a longer time at temperatures higher than 1200 °C due to transformation to equilibrium cubic (fluorite structure) and tetragonal phases ($t' \rightarrow t + c$) [5]. Upon cooling, the transformable tetragonal phase (t) undergoes a martensitic phase transformation to monoclinic phase ($t \rightarrow m$), accompanied by a catastrophic volume expansion of 4–5%. Adding a “third oxide” can stabilize the microstructure of 7YSZ upon cooling and prevent the formation of monoclinic phase [6]. Oxide doping using alternatives to yttria into ZrO_2 has also been considered. One such system is PSZ with 5 mol% CaO in ZrO_2 (CaSZ). This has been considered for applications such as oxygen sensors, and oxygen pumps in inert gases or for electrolytes in solid oxide fuel cells [7]. CaSZ can also be used as a TBC owing to its high toughness and thermal shock resistance. The only concern was the presence of $m\text{-ZrO}_2$ in CaSZ system as minor phase [8, 9].

This study has studied the thermal stability of CaSZ in terms of variation in $m\text{-ZrO}_2$ content with temperature. In order to obtain a system without an $m\text{-ZrO}_2$ phase, a completely new system of fully stabilized ZrO_2 with Ca and Y co-doping (CaYSZ) has been synthesized. However, it should be noted that fully stabilized ZrO_2 lacks a toughening mechanism and therefore crack growth will be fast in this material [10]. Since crack growth mainly occurs

A. K. Bhattacharya (✉) · P. Reinhard · W. Steurer · V. Shklover
Department of Materials, ETH Zurich, 8093 Zurich, Switzerland
e-mail: anup.bhattacharya@mat.ethz.ch

at TBC/bondcoat interface, fully stabilized ZrO_2 can be used in the outer layer of a TBC system, where crack growth is not (or less) expected to occur [11]. Again, as CaYSZ is already stabilized with Ca ions, it may reduce the reactivity of this system with airborne impurities containing Ca ion, such as CMAS. Thus, this system may have an advantage over another well studied fully stabilized ZrO_2 with Y ions (14YSZ). A detailed description of the synthesis process has been provided. A stepwise characterization of the synthesis process using X-ray diffraction (XRD) has been discussed. A comparison has also been drawn discussing the advantages and limitations of using either wet chemical or solid-state synthesis for obtaining CaYSZ.

Experimental

Commercial CaSZ (5 mol% CaO in ZrO_2) and 7YSZ from HC Strak GmbH, Germany were used in this study.

Wet chemical synthesis

CaYSZ (5 mol% CaO and 10 mol% Y_2O_3 in zirconia lattice) was synthesized through reverse coprecipitation of the metal salts in basic solutions. Appropriate amounts of calcium chloride ($\text{CaCl}_2 \cdot \text{H}_2\text{O}$, 99+% for analysis, ACROS Organics), yttrium nitrate [$\text{Y}(\text{NO}_3)_3 \cdot \text{H}_2\text{O}$, 99.9% REO, Alfa Aesar], and zirconium oxychloride ($\text{ZrOCl}_2 \cdot \text{H}_2\text{O}$, 99.9% metal basis, Alfa Aesar) were dissolved separately in 100 mL of deionized water and then mixed together. The metal salts solution was then slowly added to the precipitating basic solution under constant stirring. Two different precipitating agents were used. In the first wet chemical synthesis (chem1), an aqueous ammonia solution (ammonia solution 25%, GR for analysis, Merck) was used as a precipitating agent. A second wet chemical route (chem2) was tested, using sodium hydroxide solution as a precipitating agent. The pH of the precipitating solution was constantly maintained at 11. The gel-like precipitate obtained was filtered and washed with deionized water. The precipitate was then dried over night at 80 °C, grounded and pressed into pellets, and calcined for 4 h at 1000 °C with a heating and cooling rate of 10 K/min.

Solid state synthesis

Appropriate amounts of calcium carbonate (CaCO_3 , Puratronic® 99.997% metal basis, Alfa Aesar), yttrium oxide (Y_2O_3 , REactan® REO 99.999%, Alfa Aesar), and zirconium oxide (ZrO_2 , Puratronic® 99.978%, Alfa Aesar) were put into a Teflon bottle with zirconium oxide milling balls of 3 mm diameter (16 times the weight of the

overall powder). Ethanol (absolute ethanol, Pro analysis, Merck) was added until the bottle was halfway filled. The bottle was sealed and the contents were ball milled for 24 h at a rate of 30 spins per minute. The milled powder (sol1) was filtered and dried overnight. Dried powder was grounded, uniaxially pressed, and calcined for 6 and 10 h at 1000 °C.

Heat treatment

To study the influence of dwelling time and temperature on the phase formation and to study the sintering behavior, calcined powders from the chem1, chem2, and sol1 were uniaxially pressed into pellets and heat treated at different temperatures from 1100 to 1600 °C for durations ranging from 4 to 36 h. The goal was to obtain single-phase CaYSZ powders with minimum monoclinic phase.

Powder characterization

Phases formed by different thermal treatments were analyzed by X-ray powder diffraction (XRD, XPert Pro PANalytical, Netherlands). The measurements were done under 37 kV voltage and 45 mA current using $\text{CuK}\alpha$ radiation. Data were recorded by measuring at a 2Θ step size of 0.008° and at 100 s time per step. The scan speed was 0.01°/min in a range of $2\theta = 15\text{--}100^\circ$. Phases were identified using ICSD database. The percentage of monoclinic phase was calculated using relative integrated intensity of the characteristic diffraction peaks according to method used by Toraya et al. [12] for the monoclinic-cubic system. Powder morphology and grain size were investigated by scanning electron microscope, SEM (LEO 1530, Carl Zeiss SMT AG, Oberkochen, Germany) coupled with an energy dispersive X-ray spectrometer (EDX) for elemental analysis. All obtained powders were sputtered with carbon for SEM analysis. The following designations of the obtained CaYSZ samples are used throughout this article.

CHxCyAzT and SS1CyAzT: where prefix CHx stands for chem1 ($x = 1$) and chem2 ($x = 2$), SS1 stands for solid state route (sol1); middle C stands for calcinations at 1000 °C, y stand for duration of calcinations; A stands for annealing followed by calcinations, z stands for annealing time and suffix T denotes the temperature of annealing. If annealing is done at 1600 °C, suffix T is not given.

Sintering and coefficient of thermal expansion (CTE) of the obtained single-phase powder were also investigated through dilatometry (DIL 402C, Netzsch GmbH & Co. Holding KG, Selb, Germany). Pellets of single-phase CaYSZ powders were formed by uniaxial pressing followed by annealing at 1250 °C for 4 h for dilatometry. All the pellets were found to have relative density around 70–72%.

Results and discussion

XRD analysis of commercially obtained CaSZ shows the presence of cubic phase along with minor $m\text{-ZrO}_2$ (1.37 vol%). However, the monoclinic content increased to 23 vol% after 600 h treatment at 1250 °C. XRD patterns of CaSZ before and after the treatment are shown in Fig. 1. Such a huge increase of monoclinic phase content is highly undesirable for TBC application, hence the need for further stabilization of the system arises, so that a single phase system free of any $m\text{-ZrO}_2$ is formed. In order to achieve that, yttria was doped into the CaSZ system. The results of CaYSZ synthesis steps are discussed below.

Wet chemical synthesis of CaYSZ

Nanocrystalline CaYSZ is obtained by wet chemical synthesis as can be seen by the broad diffraction peaks of CH1C4 sample in Fig. 2. Crystallite size was calculated using the Scherer formula of the calcined powders which were ~30 and ~140 nm for chem1 (NH_4OH precipitating agent) and chem2 (NaOH precipitating agent), respectively. The growth of the crystallites, upon annealing the powders at higher temperature of 1400 °C for 4 h, is evident by the peak sharpening in Fig. 2. Phase analysis of chem1 and chem2 samples from the XRD patterns shows presence of single cubic phase ($\text{Fm}\bar{3}m$, fluorite). The lattice constants for chem1 and chem2 samples were found to be 5.1380(1) and 5.1390(1) Å, respectively. The addition of Calcia or Yttria into zirconia should increase the lattice parameter as ionic radii of Ca^{2+} (1.12 Å) and Y^{3+} (1.019 Å) ions are bigger than that of Zr ion (0.84 Å) in eight-fold co-ordination [13]. Table 1 gives the elemental compositions of chem1 and chem2 samples. Despite the higher Ca^{2+} ion content in chem2 compared to that in

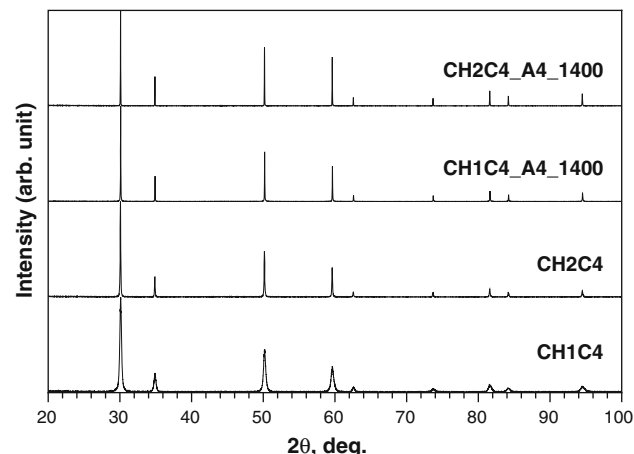


Fig. 2 XRD patterns of CaYSZ samples obtained by wet chemical synthesis: calcined (CH1C4, CH2C4) and annealed powders (CH1C4_A4_1400, CH2C4_A4_1400)

Table 1 EDX analyses (at.%) of the samples obtained by wet chemical synthesis

Sample	Zr	Y	Ca
CH1C4_A4_1400	80.54	17.69	1.77
CH2C4_A4_1400	79.54	11.04	9.42

chem1, the lattice constants are in fact equal, probably because the yttria content is higher in the chem1 sample compared to that in the chem2 sample. In a later section of this paper, an empirical relation has been deducted for the dependence of the lattice parameter of the cubic CaYSZ on the individual Ca^{2+} and Y^{3+} ion concentrations using the lattice parameters of different systems obtained in this study.

Solid-state synthesis of CaYSZ

In contrast to the samples synthesized by wet chemical route, CaYSZ powders obtained from solid-state synthesis were not single-phase after calcination. Phase evolution with different calcination time and different annealing steps are demonstrated in Fig. 3. A schematic is also presented in Fig. 4 describing stages of the solid state synthesis. The major phase observed in the calcined samples was $m\text{-ZrO}_2$ along with Y_2O_3 , cubic CaYSZ and orthorhombic CaZrO_3 (Figs. 3a, 4II). With increased calcinations time from 6 to 10 h, the peak intensity of both the CaYSZ and CaZrO_3 increases (Fig. 3b). Samples, calcinated for 6 h, show a significant decrease in the intensity of the orthorhombic CaZrO_3 peaks with further heat treatment at higher temperatures, which finally disappear at 1400 °C. The intensity of Yttria peaks also decreases with temperature and disappear at 1400 °C indicating complete

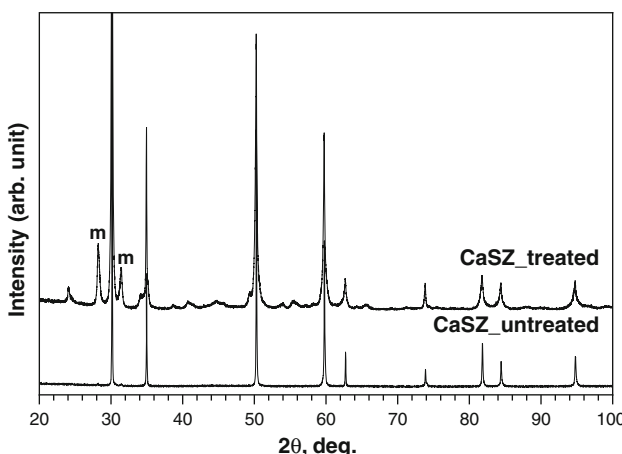


Fig. 1 XRD patterns of CaSZ sample before and after heat treatment at 1250 °C for 600 h. Diffraction peaks of $m\text{-ZrO}_2$ (m) are indicated

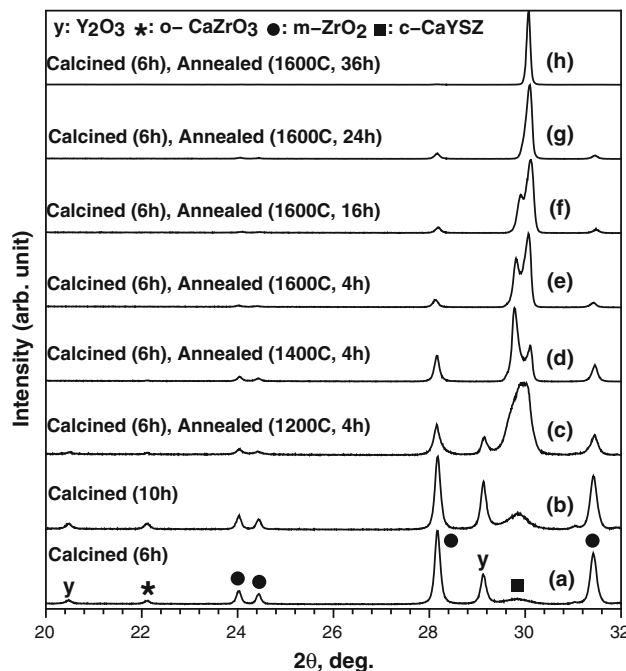


Fig. 3 XRD patterns of CaYSZ samples at different stages of calcinations and annealing obtained during solid-state synthesis (2θ -range 20–32° is shown)

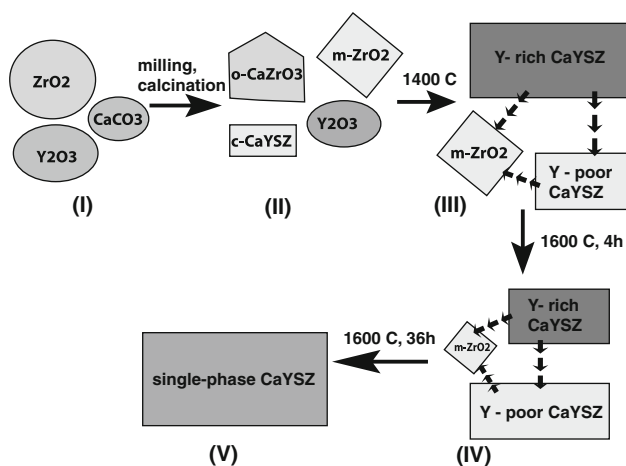


Fig. 4 Schematic showing the formation steps of CaYSZ by solid-state synthesis

dissolution of yttria in the cubic CaYSZ. With the increase in temperature, the CaYSZ peak grows and then splits into two peaks (Figs. 3d, 4III). Splitting is clearly visible at $2\theta = 30^\circ$ in the diffraction pattern of the sample that was heat treated at 1400 °C. These two peaks at $2\theta = 30^\circ$ may correspond to two different cubic CaYSZ phases with different lattice parameters. The switching of the intensity of these two peaks is seen after a 4 h heat treatment at 1600 °C (Figs. 3e, 4IV) indicating a change in the concentration ratio between both the cubic phases. Also, a

decrease in $m\text{-ZrO}_2$ content is observed. With a longer heat treatment at 1600 °C, these two peaks come closer and finally converge after a 36 h heat treatment indicating the formation of a single cubic phase (Figs. 3g, 4V). Splitting of the broad CaYSZ peaks into two clear peaks, followed by switching of intensities and finally convergence, indicate diffusion-controlled reactions in this system. The cations interdiffusion between the two cubic lattices and the rest $m\text{-ZrO}_2$ lattice finally leads to a single-phase cubic CaYSZ. The broken arrows in Fig. 4 show the diffusion of dopant ions and their direction. It can be assumed that equilibrium is reached only after a 36 h of heat treatment at 1600 °C.

The single-phase formation of CaYSZ was found to need around 72 h of heat treatment at 1600 °C, for samples calcined for 10 h, and only 36 h of heat treatment at 1600 °C for samples calcined for 6 h. This may be due to a greater presence of CaZrO_3 phase in the 10 h calcined sample. Furthermore, the formation of a third transient cubic phase could have resulted from the $o\text{-CaZrO}_3$ phase due to diffusion of Calcia from the orthorhombic lattice. Hence, a longer heat treatment (72 h, 1600 °C) was required to reach the single equilibrium cubic phase from the three different transient cubic zones.

When treated for less than 36 h, two different CaYSZ phases were present in the multiple phase samples: one high-yttria content phase and one low-yttria content phase (see Fig. 4III–IV). This is shown with the EDX analysis, as tabulated in Table 2, for the samples obtained by solid-state synthesis and annealed at 1600 °C for up to 36 h. Elemental compositions show the cubic structure of these two phases (as confirmed by the available phase diagram in Fig. 5 [14]) and these contribute to the broad peak at $2\theta = 30^\circ$ in Fig. 3g. After 36 h heat treatment, only a single-phase matrix was found whose composition matches well to the target CaYSZ composition.

The increase of Ca^{2+} or Y^{3+} dopant concentration leads to a larger cell constant, which in turn leads to a shift of diffraction peaks to a lower 2θ . Hence, the two split peaks in Fig. 3d, e, and f at around $2\theta = 30^\circ$ can be denoted to Y-rich and Y-poor cubic CaYSZ phases. With further heat

Table 2 EDX analyses (at.%) of CaYSZ samples obtained by solid-state synthesis which were calcined for 6 h at 1000 °C and then heat treated at 1600 °C for 16, 24 and 36 h. Y-deficient and Y-rich zones are analyzed

Sample	Y-deficient zone			Y-rich zone		
	Ca	Y	Zr	Ca	Y	Zr
SS1C6_A16	3.27	17.97	78.76	1.09	36.64	62.27
SS1C6_A24	7.3	11.5	81.2	1.455	30.17	68.375
SS1C6_A36	4.75	16.6	78.65			

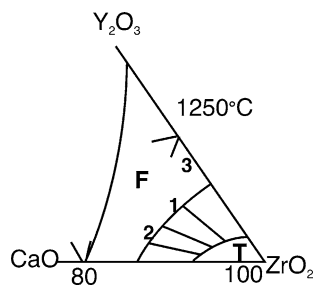


Fig. 5 Section of tentative phase diagram CaO–Y₂O₃–ZrO₂ [12], *F* fluorite phase, *T* tetragonal and 1, 2, 3 are the points corresponding to the sample compositions synthesized in this study

treatment, the doping composition equilibrates through interdiffusion of the Y³⁺ and Ca²⁺ ions (Fig. 4III–IV) and the lattice parameter becomes more homogeneous. This leads to the convergence of two cubic phases into one after 36 h treatment at 1600 °C.

The XRD patterns of single-phase CaYSZ powders, obtained by solid-state synthesis and wet chemical synthesis are shown in Fig. 6. Only the most intense part of XRD patterns, the peak at $2\theta = 30^\circ$, is shown. All of these samples have a cubic structure. Peaks of the sample calcined for 10 h are broader compared to that for the sample calcined for 6 h. The reason is again as mentioned before: homogenization didn't complete in SS1C10_A36. Delayed homogenization was due to the higher CaZrO₃ content in the longer calcined sample. By using nano-powders as starting powders, obtained by wet chemistry route, it is possible to reduce the diffusion paths and therefore the time and temperature, to 4 h and 1400 °C, needed to obtain a homogeneous composition in the case of chemical synthesis. According to Andrievskaya et al. [14], who studied the phase diagram of the CaO–Y₂O₃–ZrO₂ system first, the time needed for a solid solution to form at equilibrium is much longer than 36 h. In their study, powders were annealed for 2000 h in a furnace at 1250 °C to obtain a homogeneous sample. In our study, a homogeneous single-phase composition was obtained at 1600 °C in just 36 h. Unlike CaSZ, the CaYSZ system synthesized in this study is stable at 1250 °C for 600 h. The samples SS1C6_A36 and SS1C10_A36 contain minor m-ZrO₂ as secondary phase (~1.31 vol%) and no increase in the monoclinic phase content was observed after 600 h heat treatment at 1250 °C, indicating that addition of Yttria has stabilized the CaSZ system.

The XRD patterns in Fig. 6 also show that peaks of all the synthesized CaYSZ are shifted to lower 2θ angles compared to the CaSZ sample. This shift is due to higher dopant concentration in the CaYSZ samples. Higher dopant concentration increases the lattice parameters, and hence creates larger shift of diffraction peaks. Samples obtained by solid-state synthesis have larger lattice constants

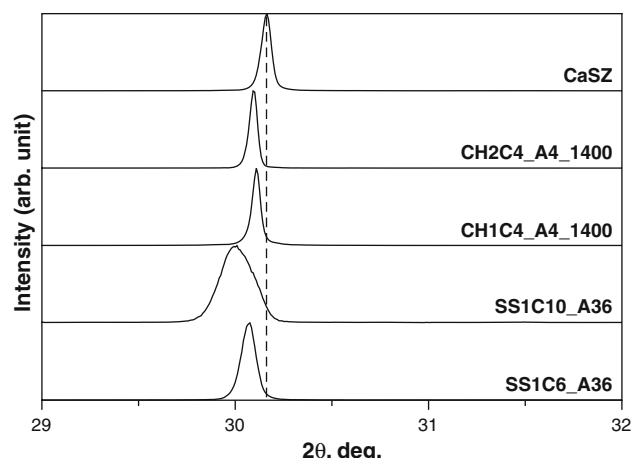


Fig. 6 XRD patterns of all single phase CaYSZ powders and CaSZ powder. Only the 111 peak is shown to highlight the relative peak positions in each system

[5.1430(1) Å for SS1C6_A36 and 5.1590(1) Å for SS1C10_A36] than samples obtained by wet chemical route [5.1380(1) Å for CH1C4_A4_1400 and 5.1390(1) Å for CH2C4_A4_1400] and also compared to commercially obtained CaSZ [5.1290(1) Å]. Introducing Y³⁺ into CaSZ increases the lattice constants of CaSZ. CH1C4_A4_1400 sample has the smallest lattice constant value among all the CaYSZ samples due to lower Ca²⁺ content. The Ca²⁺ ion is the largest cation present in the solid solution and its absence should have the strongest influence on lattice constants.

The dependence of cation concentration on the CaYSZ lattice parameter can be written as:

$$l = l_0 + m[\text{Ca}^{2+}] + n[\text{Y}^{3+}] \quad (1)$$

Here, l is the lattice parameter, l_0 is a constant that should correspond to the lattice constant of undoped cubic ZrO₂, m and n are the contributions of Ca²⁺ and Y³⁺, respectively. Putting together the EDX calculations (Tables 1, 2) and the lattice parameters calculated from the XRD patterns, it was found that $m = 19.625 \times 10^{-4}$ and $n = 9.225 \times 10^{-4}$. Putting these values for the CaSZ system where $[\text{Ca}^{2+}] = 0.05$ and $l = 5.129$ Å, l_0 value obtained was 5.128 Å, which is the value reported for cubic ZrO₂ [ICSD: 00-049-1642]. This confirms the validity of the Eq. (1) and the m and n values obtained thereafter. The m and n values obtained from this study can be used for calculation of the lattice parameters for different CaYSZ systems with different Ca and Y content. A plot of the calculated lattice parameters versus reported ones has been shown in Fig. 7. The calculated lattice parameters match well with the reported ones when only [Y³⁺] is a variable. However, huge mismatch is seen between the calculated and reported values for the Ca²⁺ ion concentration effects.

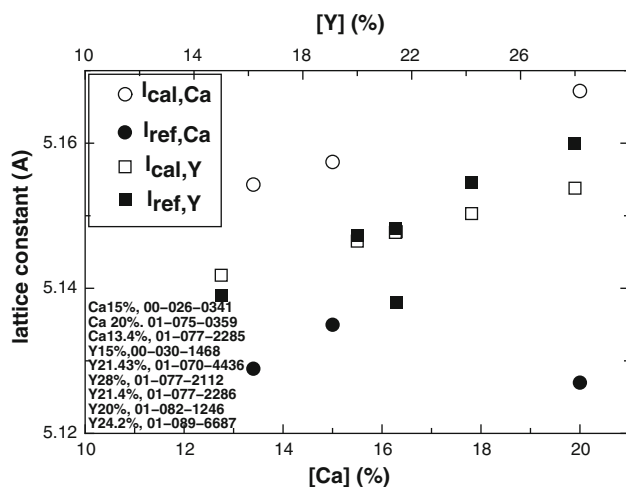


Fig. 7 A plot showing the effect of Ca and Y concentration on the lattice constant of the cubic Ca and/or Y stabilized ZrO_2 . Circles are data for the effect of Ca ion and squares are that of Y ion. Open shapes indicate the calculated values using Eq. 1 and filled shapes correspond to the published works. ICSD reference number is indicated in the bottom left corner

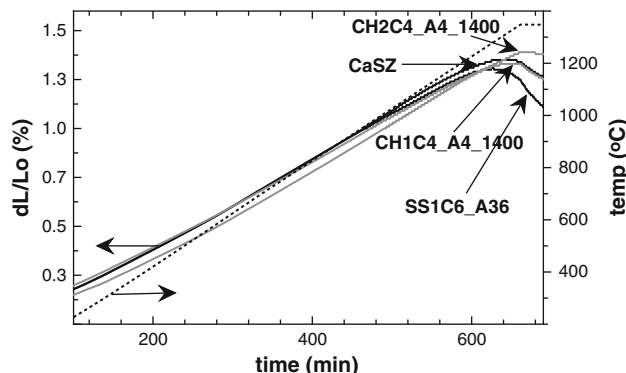


Fig. 8 Dilatometry curves showing the sintering behavior of the CaYSZ systems. Sintering rate is assumed from the slope of the curve after reaching the sintering temperature

Further studies are needed to validate this equation in terms of effect of Ca^{2+} ion on lattice parameters.

Sintering curves for the different Ca(Y)SZ samples are shown in Fig. 8. The rate of sintering of CH1C4_A4_1400 was higher than that of CH2C4_A4_1400. The Chem2 sample shows almost no sintering at 1350 °C. A higher sintering rate of the chem1 sample could be due to smaller grain size ($\sim 7.8 \mu\text{m}$) compared to that of the chem2 ($\sim 8.9 \mu\text{m}$) sample. On the other hand, though CaSZ and solid state synthesized samples have similar grain size ($\sim 15 \mu\text{m}$), SS1C6_A36 sample was found to have a higher sintering rate compared to CaSZ. This could be due to higher yttria concentration in the former. The CTE calculated for the CaYSZ system was $9.92(7) \times 10^{-6} \text{ K}^{-1}$

which is almost equivalent to that of 7YSZ ($10.21(4) \times 10^{-6} \text{ K}^{-1}$), also determined in this study.

Conclusions

Single phase CaYSZ was successfully synthesized through both wet chemical route and solid-state route. Wet chemical synthesis was faster and the particle size can be tailored by optimizing the synthesis parameters. For solid-state synthesis, equilibrium was achieved after 36 h of heat treatment at 1600 °C. Below 1600 °C and before 36 h at this temperature, two or more cubic phases are observed which can be considered as non-equilibrium phases. No monoclinic phase was found in the chemically synthesized powders and only negligible amount (1.31 vol%) was observed in the sample obtained by solid-state synthesis. Synthesized CaYSZ system shows high stability at 1250 °C for 600 h with no increase of secondary $m\text{-ZrO}_2$ phase observed with long term heat treatment. The promotion of the sintering rate by higher dopant concentration was observed. The CTE of CaYSZ system was found to be similar to that of 7YSZ.

Acknowledgements Authors would like to thank Dr. O. Fabrichnaya for important suggestions. Authors would also like to thank Dr. G. Witz for useful suggestions and discussions. Authors are indebted to Innovation Promotion Agency (CTI) of Swiss Federal Office for Professional Education and Technology (Project 8974.1 PFIW-IW) for financial support.

References

1. Schulz U (2000) J Am Ceram Soc 83(4):904
2. Jones RL (1997) J Therm Spray Technol 6(1):77
3. Clarke DR, Levi CG (2003) Annu Rev Mater Res 33:383
4. Huang X, Zakurdaev A, Wang D (2008) J Mater Sci 43:2631. doi:10.1007/s10853-008-2480-x
5. Brandon JR, Taylor R (1991) Surf Coat Technol 46:75
6. Nicholls JR, Lawson KJ (2002) Surf Coat Technol 151–152:383
7. Jayannathan KP, Tiku SK, Ray HS, Ghosh A, Subbarao EC (1980) Solid electrolytes and their applications. Plenum Press, New York, p 201
8. Garvie RC, Nicholson PS (1972) J Am Ceram Soc 55(6):303
9. Green DJ, Maki DR, Nicholson PS (1974) J Am Ceram Soc 57(3):136
10. Hannink RHJ, Kelly PM, Muddle BC (2000) J Am Ceram Soc 83(3):461
11. Kraemer S, Faulhaber S, Chambers M, Clarke DR, Levi CG, Hutchinson JW, Evans AG (2008) Mater Sci Eng A 490:26
12. Toraya H, Yoshimura M, Somiya S (1984) J Am Ceram Soc 67:C183
13. Shannon RD (1976) Acta Cryst A32:751
14. Andrievskaya ER, Kir'yakova IE, Lopato LM (1991) Inorg Mater 27(10):1839